I was engrossed in my discovery of two velocities in the case of parallel surface conductors, the second part of this paper. Its publication was delayed for three years. I failed to notice the much more important implications of the first part, which I only realised and published 43 years later, see http://www.ivorcatt.co.uk/x111.htm . In Figures 16 and 17 below, we see a third mode, neither Even Mode nor Odd Mode. The superposition of Even Mode and Odd Mode, where electric current flows in both directions along the passive line, is illegal under classical electromagnetic theory. This directs us to Theory C. http://www.ivorcatt.com/2608.htm .

Ivor Catt. April 2011

IEEE TRANSACTIONS ON ELECTRONIC COMPUTERS, DECEMBER 1967

Crosstalk (Noise) in Digital Systems

IVOR CATT

Abstract—As digital system speeds increase and their sizes diminish, it becomes increasingly important to understand the mechanism of signal crosstalk (noise) in interconnections between logic elements. The worst case is when two wires run parallel for a long distance. Past literature has been unsuccessful in explaining crosstalk between parallel wires above a ground plane, because it was assumed that only one signal propagation velocity was involved.

This paper proves that a signal introduced at one end of a printed wire above a ground plane in the presence of a second parallel (passive) wire must break up into two signals traveling at different velocities. The serious crosstalk implications are examined.

The new terms *slow crosstalk* (SX), *fast crosstalk* (FX) and *differential crosstalk* (DX) are defined.

Index Terms—Crosstalk (noise) in digital systems, Directional Couplers, graphs of characteristic impedance and crosstalk in Stripline and Microstrip, interconnection of 1-ns logic gates, multilayer printed circuit boards, resistive paper analog for measuring *L*, *C* and *Z*.

I. Introduction

THE PROPAGATION delay and signal rise time of logic circuits now available are in the region of 1 ns. To gain the speed advantage that these circuits offer us, it is necessary to reduce the physical size of a system to less than one cubic foot, so that the effective speed will not be greatly reduced by propagation delays in the interconnecting lines (reference [1], page 104). The problem of how to fit all the interconnections between logic elements into such a confined space is a difficult one, and multilayer printed circuit boards seem to be necessary.

Fig. 1 shows a cross section of such a board. In order to keep signal cross coupling (noise) down to a reasonable level, (say 10 percent of signal amplitude), at least one voltage plane must separate successive layers of signal lines. At a frequency of 1 GHz, skin depth in copper (reference [2], page 238) is 2×10^{-4} cm (=0.00008 in.). At 10 GHz, skin depth drops to 7×10^{-5} cm (=0.00003 in.). At present, it is not practicable to laminate copper less thick than 0.001 in. (which is more than ten times the skin depth). This means that in practice, a signal traveling down a signal line and returning by the immediately adjacent voltage plane(s) will not penetrate beyond the plane(s), and each voltage plane will screen signals above it from signals below it with negligible crosstalk through the voltage plane. So long as a signal is transmitted down between a signal line and the voltage plane(s) immediately above or below it, the only

Manuscript received August 29, 1966; revised July 5, 1967.
The author is with Sperry Semiconductor Division, Norwalk, Conn.

crosstalk (noise) of significance will be between signal lines in the same plane. Care must be taken that at its source and destination, the signal is referenced to the correct voltage plane(s).

Depending on dielectric thickness separating voltage planes, there may be insufficient natural decoupling between voltage planes, and it may be necessary to add discrete voltage supply decoupling capacitors at intervals around the board. If a signal is introduced at a point LM between two parallel planes, Fig. 2, it travels out radially between the planes, seeing a characteristic impedance Z_0 which continually decreases as time increases and r increases (reference [2], page 395). At a radius r,

$$Z_0 = \frac{d}{2\pi r}\sqrt{\frac{\mu}{\epsilon}}\cdot$$

Now the velocity

$$c = \frac{r}{t} = \frac{1}{\sqrt{\mu\epsilon}}\cdot$$

So substituting for r,

$$Z_0 = \frac{d\mu}{2\pi t}\cdot$$

A reflection related to Z_0 arrives back at the center at time $2t$. If Z_0 is small when $2t = t_r$, then natural decoupling between planes is satisfactory.

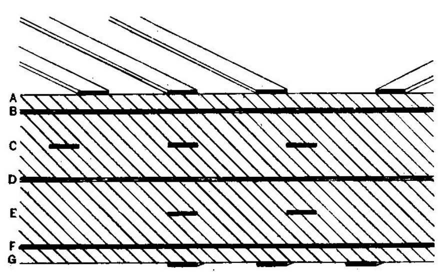

Fig. 1. Cross section of a multilayer printed circuit board.

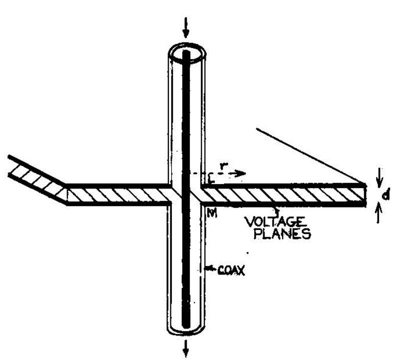

Fig. 2. A signal passing through layers of a multilayer board sees a series impedance between the planes, which reduces the amplitude of the signal continuing down the line.

As an example, if $2t = 1$ ns, $d = 0.020$ in.,

$$Z_0 = \frac{0.020 \times 4\pi \times 10^{-7}}{2\pi \cdot 1/2 \cdot 10^{-9}} = 4 \text{ ohms}.$$

This calculation shows that it is possible to keep the decoupling between voltage planes satisfactory by the addition of extra decoupling capacitors distributed at intervals of one or two inches, to prevent superposition of signals from generating unacceptably large voltage transients between planes.

The proportion of the surface area occupied by miniature tantalum capacitors will be insignificant.

The problem now left is signal crosstalk (noise) between signal lines in the same plane, the topic of this paper. The worst case for crosstalk between two signal lines is when they are parallel and close together; therefore the case studied in this paper is that of crosstalk (noise) between long parallel lines. The case of buried conductors (Plane C, Fig. 1) will be covered in Section II, and the case of surface conductors (Plane A, Fig. 1) will be covered in Section VI.

II. Description of Crosstalk between Parallel Buried Conductors

Fig. 24 shows a cross section of the lines under discussion. Fig. 3 shows a plan view. Fig. 4 shows a diagrammatic representation of the same.

In a computer system, a voltage-current step v, i, representing a transition from the FALSE state to the TRUE state, is introduced at A_0G_0. Lines are assumed to be lossless and so propagation is TEM. If Z_0 is the characteristic impedance between the lines A_0A_1, G_0G_1, then $v = iZ_0$.

When this signal reaches A_1G_1, the effect of the line P_1P_2 has to be considered.

If the front end P_1G_1 is open circuit, no current can flow in the line, and the only change in Z_0 will be due to the effect of charge moving in a lateral direction across the passive line. This effect may be safely neglected. If P_1G_1 is shorted, the change in Z_0 on line A which occurs at A_1G_1 is a maximum. However, if the line spacing is

Fig. 3. Plan view of parallel buried conductors.

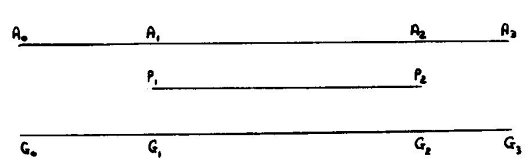

Fig. 4. Diagrammatic representation of active transmission line and passive transmission line.

such that the maximum crosstalk between lines is acceptably low, this effect may also be neglected.
[If

$$\frac{\text{maximum crosstalk}}{\text{signal}} = x,$$

then maximum change of Z_0 at A_1G_1 is by a factor $(1-x^2)$. In practice, $x<0.1$. So change of Z_0 is <0.01.]

So it may be assumed that the characteristic impedance of a line is not altered significantly by the presence of other lines.

It is not possible for a current voltage signal to travel from A_1G_1 to A_2G_2 and leave the line P_1P_2 unaffected. Two fundamental TEM modes can exist on a pair of parallel conducting strips between parallel ground planes. (reference [3], page 29)

One mode is called the Even coupled-strip Mode (EM), because the strips are at the same potential and carry equal currents in the same direction. The characteristic impedance of each line in the even mode is Z_{0e}.

The other mode is called the Odd coupled-strip Mode (OM), because the strips are at equal but opposite potentials and carry equal currents in opposite directions. The characteristic impedance of each line in the odd mode is Z_{0o} (reference [3], page 29).

$$Z_{0e} > Z_0 > Z_{0o}$$

Now the total voltage and current step passing A_1 is v, i, where $v/i = Z_0$. If P_1G_1 is open circuit, the total current passing P_1 is zero. So if the voltage–current steps continuing down the line A_1A_2 are respectively v_e, i_e, for the EM and v_o, i_o for the OM signal, then $i_e = i_o$, $v_e + v_o = v$.

Also,

$$v_e = i_e Z_{0e}$$

and

$$v_o = i_o Z_{0o}.$$

Since $i_e = i_o$ and $Z_{0e} > Z_{0o}$, $v_e > v_o$.

So the net voltage appearing on the passive line is positive and equals

$$\begin{aligned} v_{P_1G_1} &= v_e - v_o \\ &= i_e Z_{0e} - i_o Z_{0o}. \end{aligned}$$

The ratio of crosstalk amplitude to signal is

$$\begin{aligned} \frac{v_{P_1G_1}}{v} &= \frac{i_e Z_{0e} - i_o Z_{0o}}{i_e Z_{0e} + i_o Z_{0o}} \\ &= \frac{Z_{0e} - Z_{0o}}{Z_{0e} + Z_{0o}}. \end{aligned}$$

So as the signal travels down A_1A_2, a smaller crosstalk voltage step appears on the line P_1P_2. The crosstalk that is seen is the small difference between two large signals, whose sum, equal to the original signal v, i, is seen on the driven line A_1A_2. This crosstalk is here defined as fast crosstalk (FX), because its full amplitude is reached only if the signal rise time is fast compared to the propagation time down P_1P_2. The magnitude of the crosstalk so obtained is the maximum that can appear anywhere on the line P_1P_2, for any values of terminating resistors at P_1G_1 and P_2G_2. It is a good value to use for worst-case design. Fig. 24 gives values of maximum crosstalk for various cross sectional geometries.

Fast Crosstalk (FX) is a flat topped pulse whose rise and fall times equal t_r for the original signal, and whose width equals twice the propagation time down the passive line. Jarvis calls it the Backward Wave (reference [11], page 481).

Slow Crosstalk (SX) is the degenerate case of FX, when the propagation time down the passive line and back is less than t_r. SX has the triangular (noise spike) shape that we are all familiar with in slower logic.

III. Photographs of Crosstalk in Buried Conductors

Photographs were taken of waveforms generated in pairs of buried lines of various cross sectional geometries. All supported the theory contained in this paper.

In this section, waveforms taken from only one pair of transmission lines are shown. The case selected was a gross case, where FX exceeds 20 percent and the lines are very long and close together. The dimensions, shown in Fig. 5, would not be used in a practical case, but they do illustrate the theory very well. Fig. 6 shows the artwork used to make the board.

Fig. 7, third trace, shows a very narrow spike, generated by an E-H 125 pulse generator and then introduced to the front (outside) end of the active line in Figs. 6 and 5. This spike then travels down the active line. Traces 2 and 1 of Fig. 7 are taken further down the active line. Fig. 8 shows the same points on the passive line.

Figs. 9 and 10 show an enlarged view of the third trace in Figs. 7 and 8. According to the theory, these traces should be identical except in amplitude. As a further check, Fig. 11 shows the front end of the passive line on a larger voltage scale.

Fig. 12 shows the second trace of Fig. 7 superimposed on the second trace of Fig. 8. Fig. 13 shows the same, with one signal amplified. As predicted by theory, we see that the spikes on the two lines are equal except in amplitude.

Figs. 14 and 15 are a repeat of Figs. 7 and 8, but with the front end of the passive line shorted to ground. As predicted, the crosstalk voltage is now zero amplitude all down the line.

Figs. 16 and 17 show what happens if, instead of introducing a spike into the active line as shown in Figs. 7 and 8, a step is introduced.

Fig. 18 shows waveforms 120 inches down both lines when a common mode (EM) pulse is introduced at the front (outside) end of the active and passive lines in Figs. 6 and 5. In Fig. 18, each line is correctly terminated with 84 ohms, which equals Z_{0e}, so that an EM signal is not reflected. However, Fig. 19 shows what happens if only the active line is driven, leaving the front end of the passive line open circuit. The EM signal is still properly terminated, but the OM signal sees too high a termination ($Z_{0o} < Z_{0e}$) and so is partially reflected without change of polarity.

On an enlarged scale, Fig. 20 shows what happens if the reflection is reduced to zero on the active line by altering the termination resistor on the active line, while keeping the terminations on the two lines equal. A negative reflection is then obtained on the passive line. This is because with this value (70 ohms) the inverted EM reflection exactly cancels the OM reflection on the active line. However, they add rather than cancel on the passive line. So Fig. 20 shows that it is not possible to stop all reflections merely by terminating lines to ground. The way to stop all reflections is by terminating the lines and ground in a delta of resistors, Fig. 21, so that OM and EM signals will see different terminations, and each mode will be terminated correctly.

Figs. 18 through 21 indicate that the best way to look at this problem is in terms of the two modes, even and odd. This point of view will be further substantiated in Section VIII.

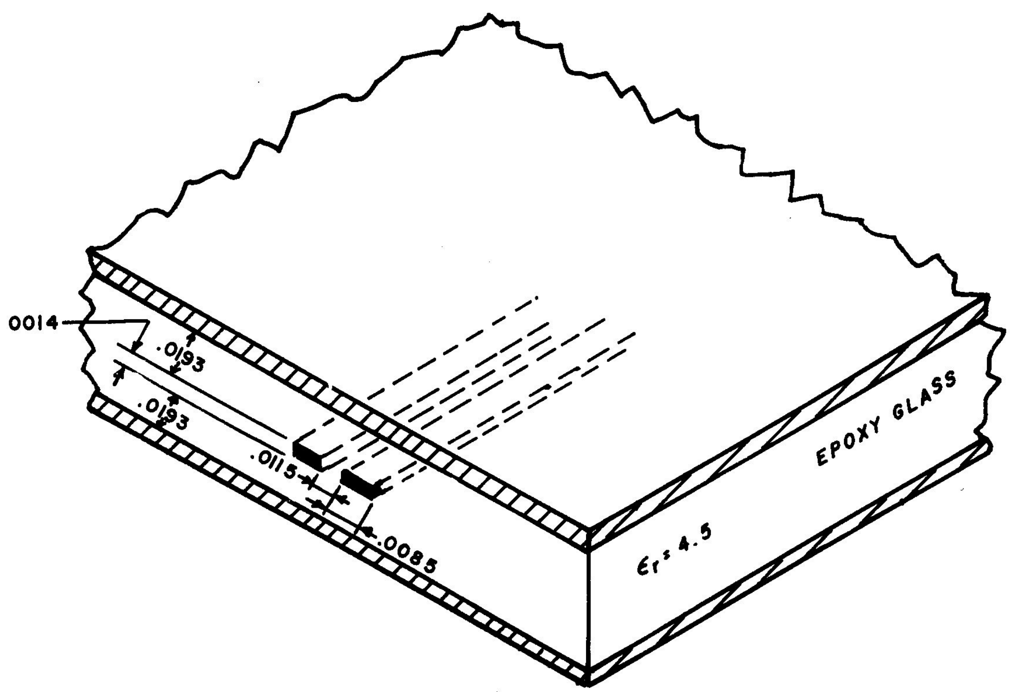

Fig. 5. Dimensions of board used to produce photographs.

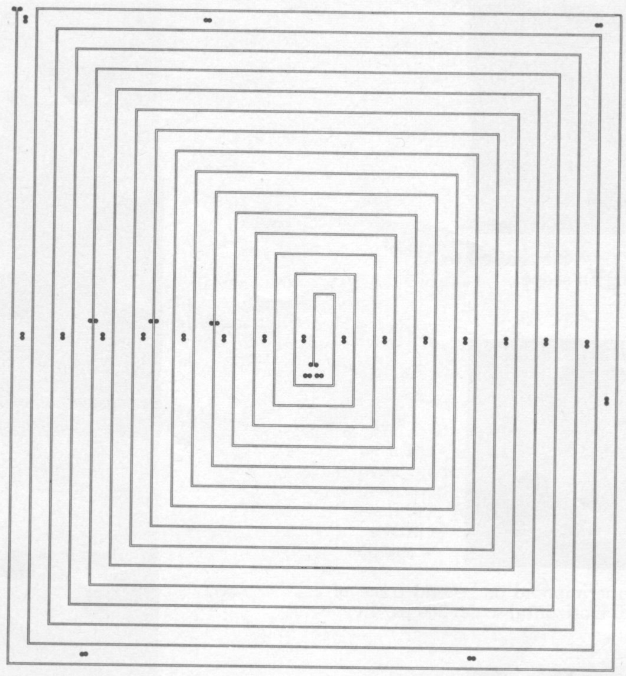

Fig. 6. Artwork used to make board (8.6 inches×7.9 inches).

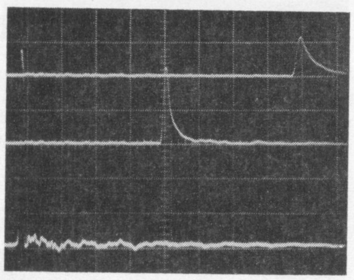

Fig. 7. Active line. Third trace: front end of line. Second trace: 120 inches down line. First trace: 234 inches down line. Vertical Scale: 20 mV/div. E-H-125 generator. 10-volt pulse through 10-dB pad into 50-ohm input of Tektronix 4S2 plug-in unit of 661 oscilloscope. Horizontal scale: 5 ns/div.

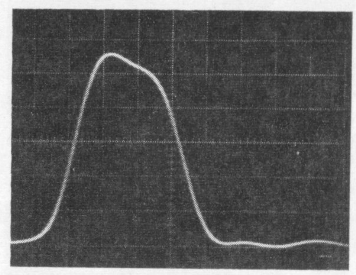

Fig. 9. Enlarged view of third trace in Fig. 7. Vertical scale: 20 mV/div. Horizontal scale: 200 ps/div.

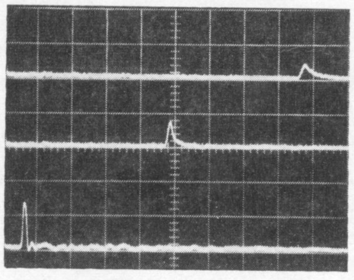

Fig. 8. Passive line. Third trace: front end of line. Second trace: 120 inches down line. First trace: 234 inches down line.

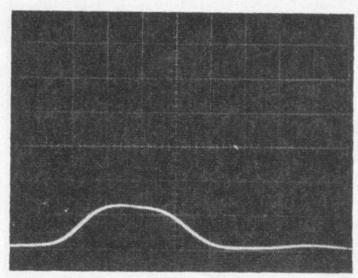

Fig. 10. Enlarged view of third trace in Fig. 8.

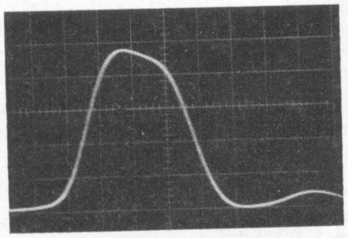

Fig. 11. Amplitude of Fig. 10 increased to 5 mV/div. setting on scope.

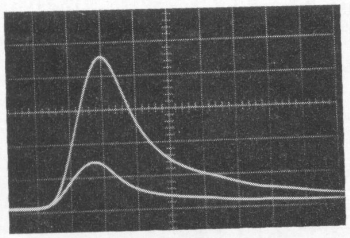

Fig. 12. Second trace of Fig. 7 superimposed on second trace of Fig. 8. Vertical scale: uncalibrated. Horizontal scale: 500 ps/div.

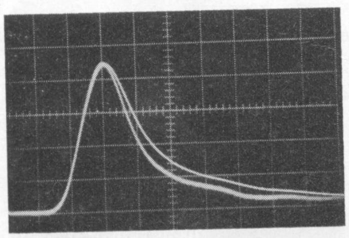

Fig. 13. Same as Fig. 12 with one trace amplified.

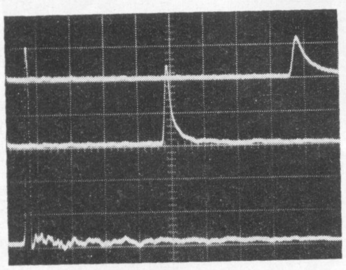

Fig. 14

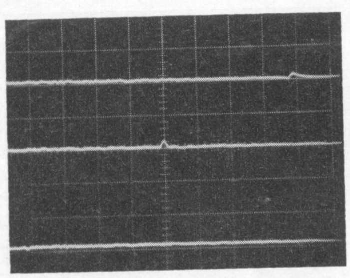

Fig. 15

Figs. 14 and 15. Same as Figs. 7 and 8 but with front end of passive line shorted to ground instead of open.

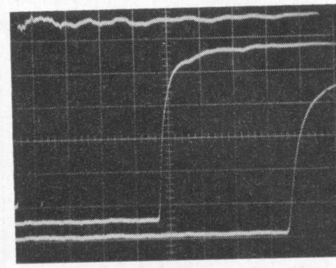

Fig. 16

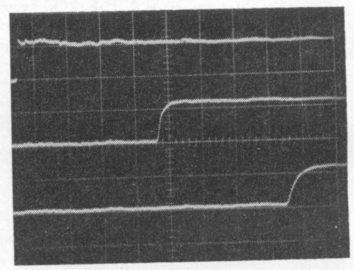

Fig. 17

Figs. 16 and 17. Same as Figs. 7 and 8 but with a step introduced into the active line instead of a narrow spike.

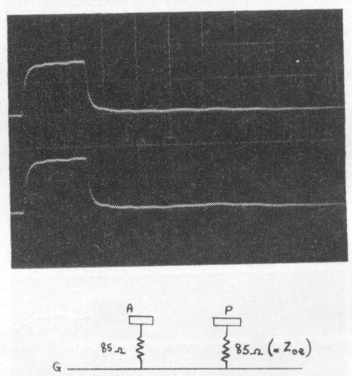

Fig. 18. Even mode pulse introduced into both lines. First trace: Active line 120 inches down line. "Active" line and "passive" line each have a termination at the far end equal to Z_{oe}(=85 ohms) so there is no reflection of the even mode pulse. Second trace: "Passive" line at same point. Vertical scale: 50 mV/div. Horizontal scale: 10 ns/div.

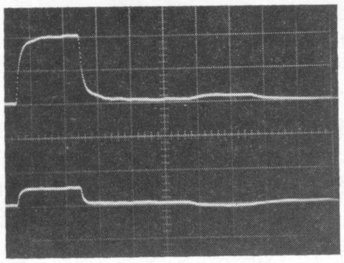

Fig. 19. Same as Fig. 18, but with active line only driven, and passive line open circuit at front end. Both lines still terminated with Z_{0e} at far end. Notice that the odd mode signal is partially reflected.

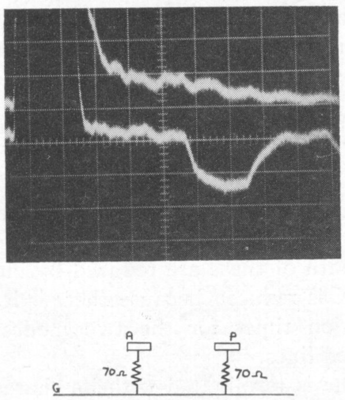

Fig. 20. Same as Fig. 19, except that both terminations have been reduced until the reflection on the active line (upper trace) disappears. Vertical scale has been increased 10× to 5 mV/div. Note that a reflection remains on the passive line.

IV. Theory of Crosstalk in Buried Lines

Cohn[3] and others[6],[12] have said that two fundamental TEM modes can exist on a pair of parallel conducting strips between parallel ground planes. (It is assumed that the system is lossless.) These modes are described in Section II. The proof that two propagation modes exist is included in Section XI and Appendix II for the case of two wires above a single ground plane, but it is equally valid for buried lines. The proof implies that any signal traveling down the pair of lines must be a combination of signals in the two modes superposed. Since the characteristic impedances, Z_{0e} and Z_{0o}, are unequal, it follows that if voltage and current in the active line A_1A_2, Fig. 4, are nonzero, then there is no case when both voltage and current in the passive line P_1P_2 are zero.

To short the front end of the passive line, P_1, to ground will not eliminate crosstalk, because although the voltage $v_{P_1G_1}$ will thus be initially clamped to zero, crosstalk current will flow along P_1P_2, resulting in voltage crosstalk at P_2G_2 after reflection of the primary waves.

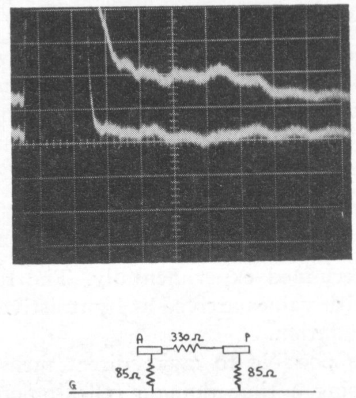

Fig. 21. Same as Fig. 20 except that the two lines are now terminated with the correct delta of resistors so that there is no reflection of even mode signals or of odd mode signals. With this delta, an even mode signal will see 85 ohms to ground at the far end of each line. An odd mode signal will see 56 ohms to ground at the far end of each line. (Half of 330 ohms in parallel with 85 ohms equals 56 ohms).

V. Methods of Determining Z_0, Z_{0e}, Z_{0o}, and Fast Crosstalk between Buried Conductors

Resistive Paper

It was found that the easiest way to determine these values was by painting electrodes onto resistive paper to represent a cross section of the two lines and also the voltage planes. (It is possible to avoid the tedium of painting voltage planes by cutting the resistive paper through the center of the conductors and then repeating the image of what remains below the now unnecessary remaining voltage plane.)

Z_0, Z_{0o}, and Z_{0e} may be measured directly using a resistance meter and applying a correction factor $(1/\rho)\sqrt{\mu/\epsilon}$, where ρ = resistance per square of the paper. To find the ratio (maximum FX)/signal, a voltage is simply placed on one line and the resulting voltage is measured on the other line. The voltage ratio gives the answer directly.

The great advantage of using resistive paper is that it avoids the cost and time delay involved in fabricating boards. The results obtained agree with those obtained by direct measurement and also with those obtained by calculation.

Calculation

Cohn (reference [3], page 29) has exact formulas for Z_{0e} and Z_{0o} for buried lines of zero thickness. He also has approximate formulas for lines of finite thickness. His results agree with the results achieved by using resistive paper and also with results of direct measurement.

Direct Measurement

Once a board has been fabricated with two long parallel buried lines, it is reasonably easy to send a voltage step down one line and measure the resulting maximum FX on the other line. So the ratio

$$\frac{\text{maximum FX}}{\text{signal}} = \frac{Z_{0e} - Z_{0o}}{Z_{0e} + Z_{0o}}$$

can be determined experimentally. The results agree very well with values arrived at by resistive paper, and also by calculation.

It is also possible to make direct measurement of Z_{0e}, $2Z_{0o}$, using a time domain reflectometer. Also, an L–C meter could be used to measure the appropriate inductances and capacitances. Unfortunately, these measurements are all likely to be inaccurate, as we are dealing either with small values or with small differences between large values.

VI. Description of Crosstalk in Surface Lines

Fig. 25 shows a cross section of the lines under discussion. Fig. 3 can serve as a plan view. Fig. 4 can serve as a diagrammatic representation of the same.

In a computer system, a voltage-current step v, i, representing a transition from the FALSE state to the TRUE state, is introduced at A_0G_0. Propagation is approximately TEM. [See Section XI]. If Z_0 is the characteristic impedance between the lines A_0A_1, G_0G_1, then $v = i\,Z_0$.

When this signal reaches A_1G_1, the effect of the line P_1P_2 has to be considered. In Section II, it is shown that the mismatch on line A at A_1 is negligible in practical cases. This is also true for surface lines. So voltage and current v, i, continue along line A past A_1.

However, as in Section II, when the signal v, i, passes A_1, it must break up into a combination of the two possible TEM modes for a pair of parallel conducting strips above a ground plane. These modes are described in Section II.

If P_1G_1 is open circuit, it was shown in Section II that the ratio of crosstalk amplitude at P_1 to signal amplitude is

$$\frac{v_{P_1G_1}}{v} = \frac{Z_{0e} - Z_{0o}}{Z_{0e} + Z_{0o}}.$$

So as the signal travels down A_1A_2, a smaller crosstalk voltage step appears at P_1. The crosstalk that is seen is the small difference between two large signals, whose sum, equal to the original signal v, i is seen on the driven line at A_1.

This crosstalk is here defined as fast crosstalk, FX, because its full amplitude is reached only if the signal rise time is fast compared to the propagation time down P_1P_2.

Unlike the case of buried conductors, the magnitude of FX is not the maximum that can appear anywhere on the line P_1P_2. The reason for this is that as surface conductors are in an inhomogeneous medium, the OM signal travels faster than the EM, (section XI. Also references [3], page 30 and [8], page 54) and so further down the line P_1P_2 the OM signal appears on its own for a time. This is here defined as Differential Crosstalk (DX) and it greatly exceeds FX. In long lines, it reaches an amplitude of approximately $v/2$, even for widely separated lines. To reach its maximum amplitude of $v/2$, the difference in propagation times for the two modes down P_1P_2 must exceed the rise time of the original signal v, i.

In practice, this is not the case, and only a fraction of the maximum possible DX appears. The actual amplitude reached by DX at P_2 is equal to

$$\frac{v}{2} \cdot \frac{(\text{difference in propagation times down } P_1P_2)}{\text{signal rise time}}.$$

In the case of surface lines, the designer should be sure that FX is not excessive and also that DX is not excessive. Both of these are reduced by increasing line spacing. DX is reduced because there is less difference in propagation times for the two modes with more widely spaced lines.

If each line is terminated with its characteristic impedance Z_0 at A_2G_2, then reflected DX will be less than FX, and so need not be considered. However, if the lines are terminated in a mismatch, such as short circuits or open circuits, then the OM signal, which arrives first at A_2P_2, will be reflected. On the way back to A_1P_1, it will draw further away from the (now reflected) EM signal. So if the lines are badly terminated, the amplitude reached by *reflected* DX when it reaches P_1 will equal

$$\frac{v}{2} \cdot \frac{(\text{difference in propagation times down } P_1P_2 \text{ and back})}{\text{signal rise time}}$$

This is double the amplitude reached by DX. However, this is not a practical case, because for reasons of reflections alone not related to crosstalk, A_2G_2 must be terminated properly. So we need only consider the case when A_2G_2 is properly terminated, either by a further length of line A_2A_3 or by a resistor Z_0, and there is only a mismatch (short or open) at P_2G_2. In that case, the incident OM signal will be reflected in two modes, half OM and half EM, and it can be shown that the maximum amplitude of *reflected* DX will be only about half the maximum DX.

The conclusion is that in practice the problem of *reflected* DX may be ignored, and one need only consider FX and DX.

VII. Graphs of Characteristic Impedance and Crosstalk

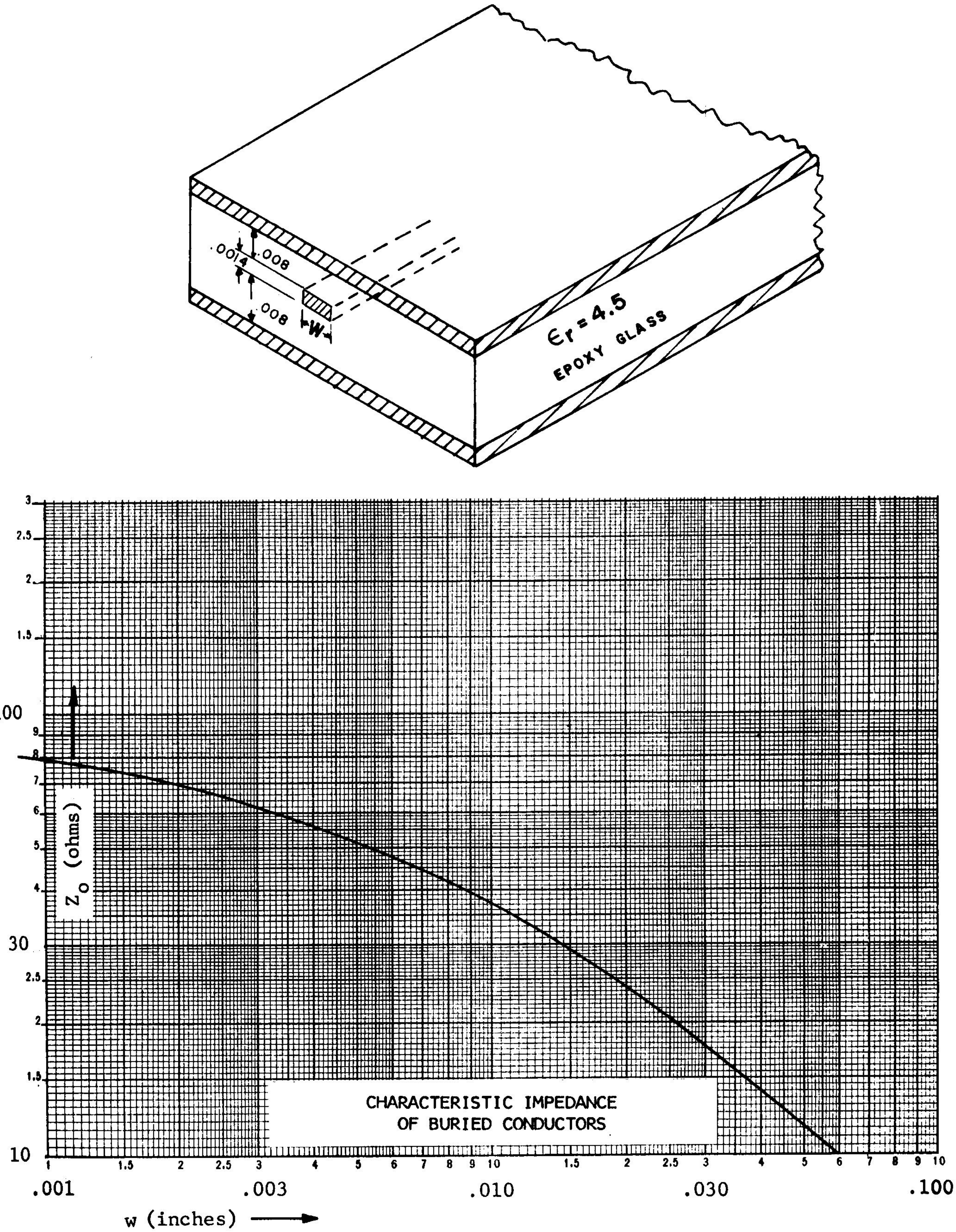

Fig. 22. Cross section of buried conductor and graph of resulting characteristic impedance.

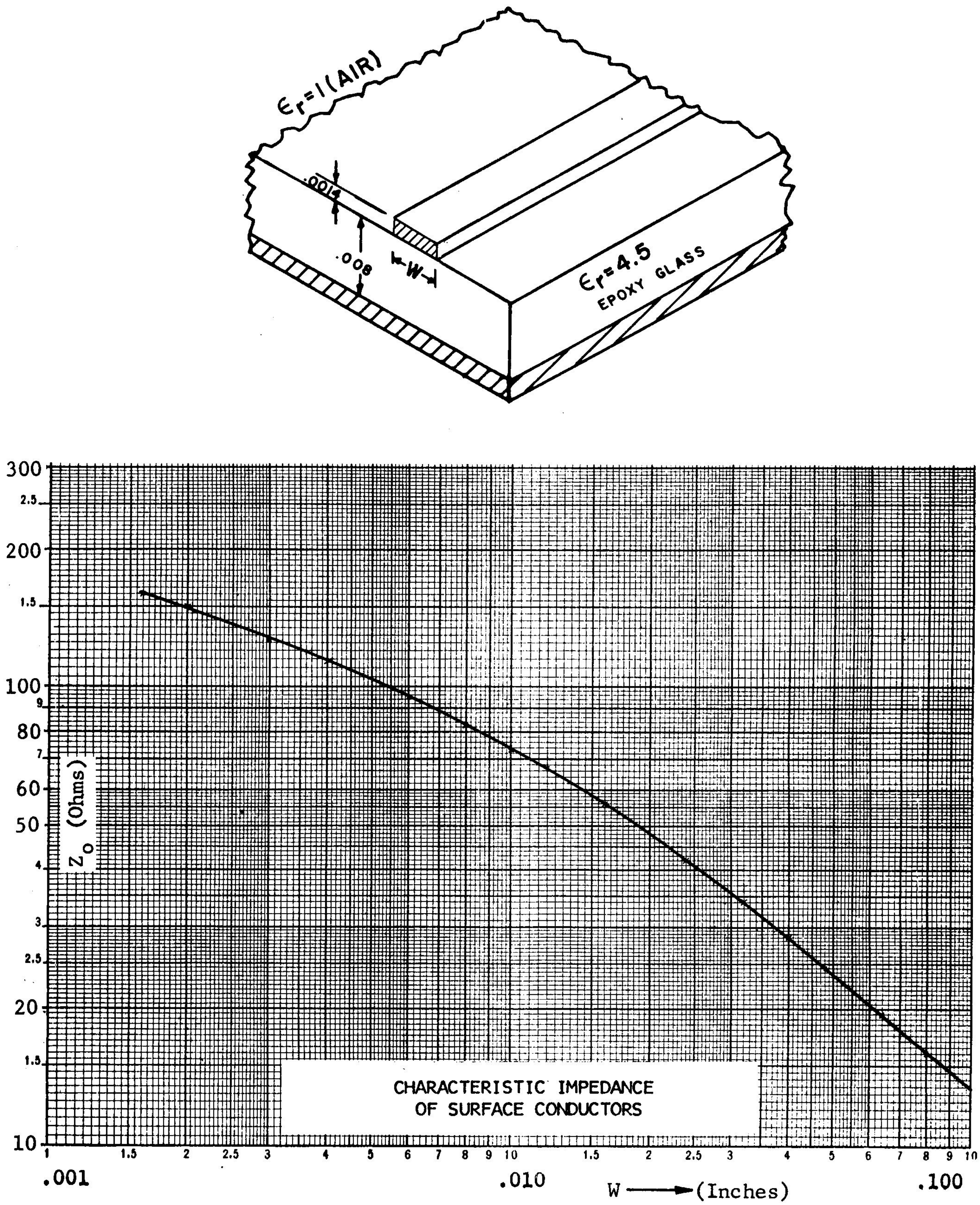

Fig. 23. Cross section of surface conductor and graph of resulting characteristic impedance.

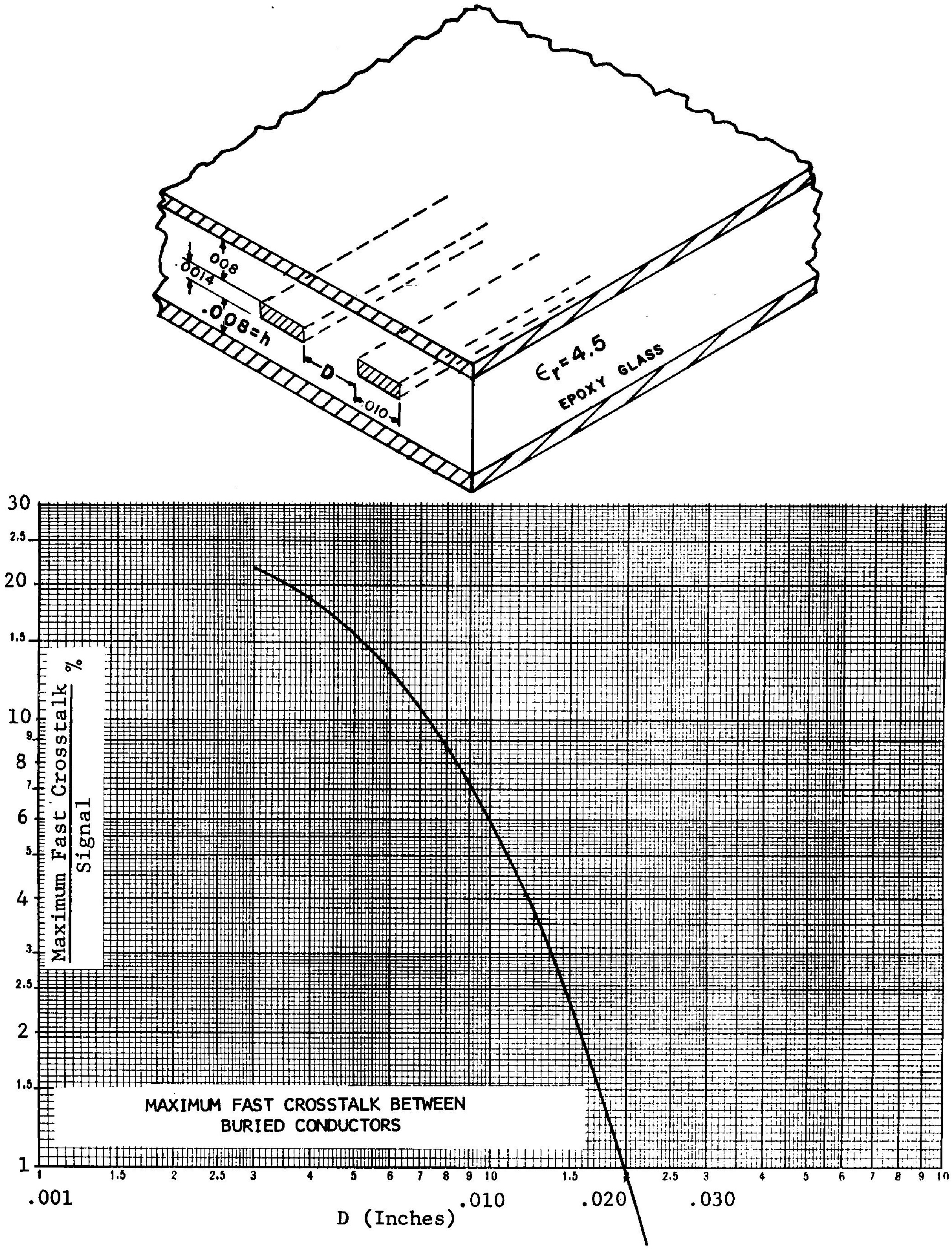

Fig. 24. Cross section of buried active transmission line and passive transmission line, and graph of resulting crosstalk (D/h may be scaled).

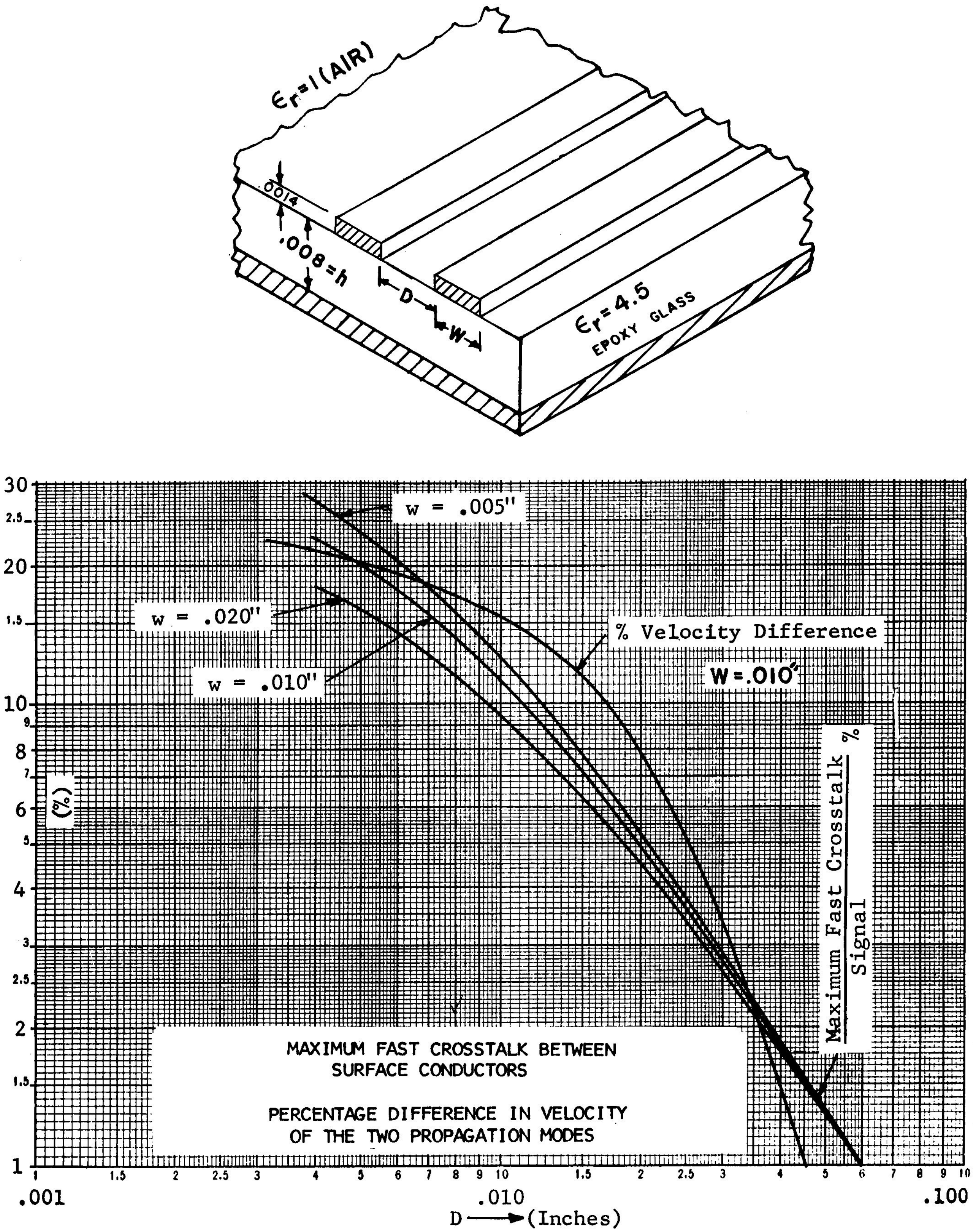

Fig. 25. Cross section of surface active transmission line and passive transmission line, and graph of resulting crosstalk (D/h may be scaled).

VIII. Photographs of Crosstalk in Surface Conductors

Photographs were taken of waveforms generated in pairs of surface lines of various cross sectional geometries. All supported the theory contained in this paper.

In this section, waveforms taken from only one pair of transmission lines are shown. The case selected was a gross case, where FX exceeds 30 percent and the lines are very long and close together. The dimensions, shown in Fig. 26, would not be used in a practical case, but they do illustrate the theory very well. Fig. 27 shows the artwork used to make the board.

Fig. 28, third trace, shows a very narrow spike, generated by an E-H 125 pulse generator and then introduced to the front (outside) end of the active line in Figs. 26 and 27. This spike then travels down the active line. Traces 2 and 1 of Fig. 28, which are taken further down the active line, show that the original spike breaks up into two spikes traveling at different velocities. The presence of the parallel passive line causes this to happen.

Figs. 30 and 31 show an enlarged view of the third trace in Figs. 28 and 29. According to the theory, these traces should be identical except in amplitude. As a further check, Fig. 32 shows the front end of the passive line on a larger voltage scale.

Fig. 33 shows the second trace of Fig. 28 superimposed on the second trace of Fig. 29. Fig. 34 shows the same, with one signal inverted. As predicted by theory, the spikes on the two lines are equal or equal and opposite.

Figs. 35 and 36 are a repeat of Figs. 28 and 29, but with the front end of the passive line shorted to ground. As predicted, the EM and OM signals are now of equal amplitude.

Figs. 37 and 38 show what happens if, instead of introducing a spike into the active line as shown in Figs. 28 and 29, a step is introduced.

Comparison of the velocity of propagation in the absence of a passive line is shown in Fig. 39. The second trace shows the time of arrival of the two spikes at the far end of the active line in the presence of a passive line. To get the first trace, a similar board was constructed without a passive line and a signal of identical amplitude and timing was introduced at the front end. This picture shows that OM propagation velocity is faster than normal, and EM propagation velocity is slower than normal velocity down a single line. This is predicted by the theory.

Reflections

Fig. 40 shows the waveforms on the active and passive lines at a point 204 inches down the lines. The far end of the lines, at distance 270 inches, is open circuit, so the signals are reflected back down the lines unchanged.

Fig. 41 shows what happens if the far end of the active and passive lines are shorted together. The OM signal sees a short, and so it is inverted on reflection. The EM signal sees an open, and so is reflected without inversion.

Fig. 42 shows that if a resistor equal to $2Z_{0o}$ is placed between the ends of the active line and passive lines, the OM signal is properly terminated and does not reflect, while the EM signal is fully reflected.

Figs. 43 and 44 show the complete suppression of reflections which results if the lines terminate with the correct delta of resistors. Comparison of Fig. 45 with 44 shows that the 300-ohm resistor definitely reduces reflections.

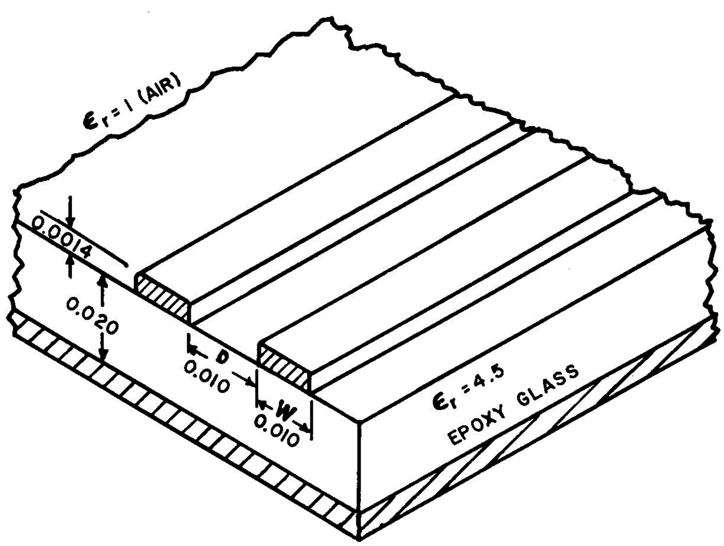

Fig. 26. Dimensions of board used to produce photographs.

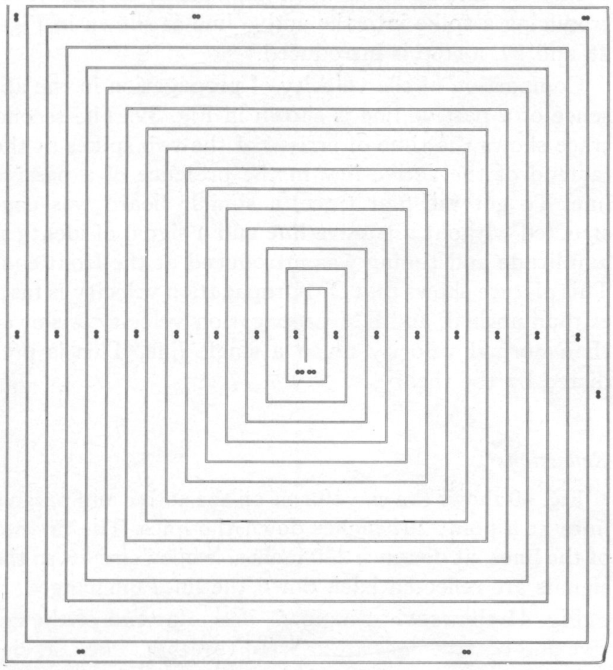

Fig. 27. Artwork used to make board (8.6 inches × 7.9 inches).

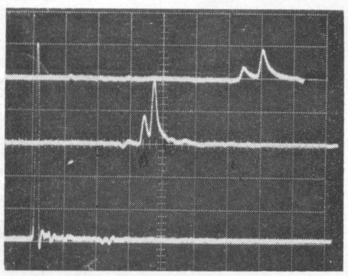

Fig. 28. Active line. Third trace: front end of line. Second trace: 120 inches down line. First trace: 234 inches down line. Vertical scale 20 mV/div. EH-125 generator. 10-volt pulse thru 10-dB pad into line. Probing by 500-ohm (10×) probe thru 10-dB pad into 50-ohm input of Tektronix 4S2 plug-in unit of 661 oscilloscope. Horizontal scale: 5 ns/div.

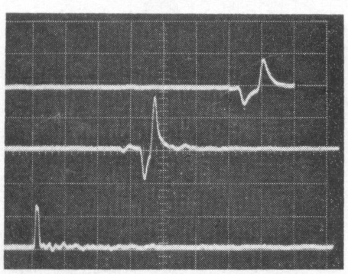

Fig. 29. Passive line. Third trace: front end of line. Second trace: 120 inches down line. First trace: 234 inches down line.

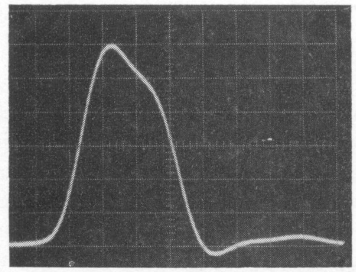

Fig. 30. Enlarged view of third trace in Fig. 28. Vertical scale: 20 mV/div. setting on scope. Horizontal scale: 200 ps/div.

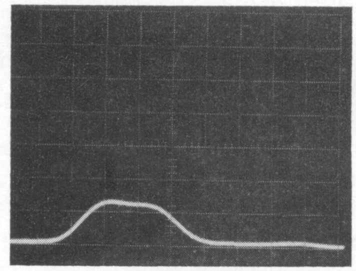

Fig. 31. Enlarged view of third trace in Fig. 29.

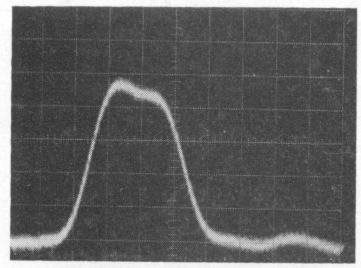

Fig. 32. Amplitude of Fig. 31 increased to 5 mV/div. setting on scope.

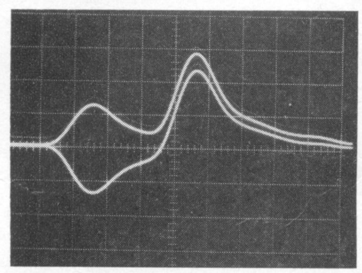

Fig. 33. Second trace of Fig. 28 superimposed on second trace of Fig. 29. Vertical scale: uncalibrated. Horizontal scale: 500 ps/div.

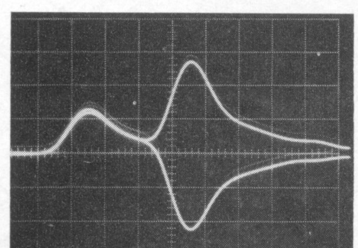

Fig. 34. Same as Fig. 33 with one trace inverted.

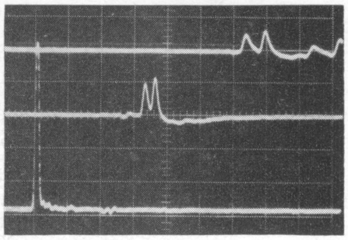

Fig. 35

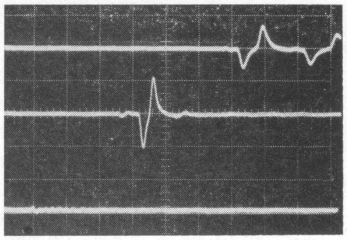

Fig. 36

Figs. 35 and 36. Same as Figs. 28 and 29 but with front end of passive line shorted to ground instead of open.

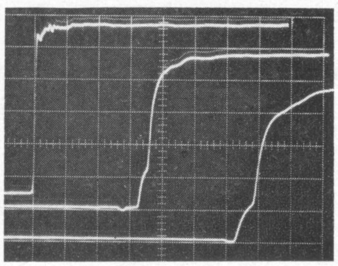

Fig. 37

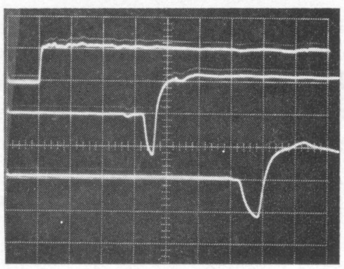

Fig. 38

Figs. 37 and 38. Same as Figs. 28 and 29 but with a step introduced into the active line instead of a narrow spike.

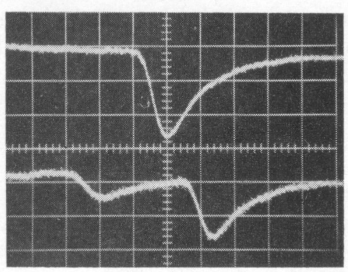

Fig. 39. Pictures taken at the far end of 270-inch-long lines (negative signals). Vertical scale: uncalibrated. Horizontal scale: 500 ps/div.

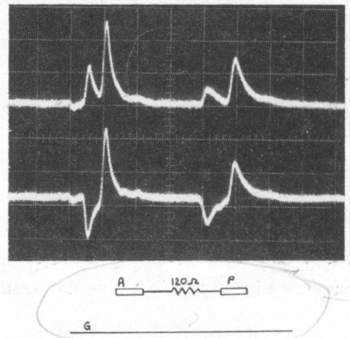

Fig. 40. First trace: active line 204 inches down line. First two spikes are signal traveling down line. Second two spikes are signal reflected back from the open circuit at 270 inches down line. Second trace: passive line. Vertical scale: 10 mV/div. Horizontal scale: 5 ns/div.

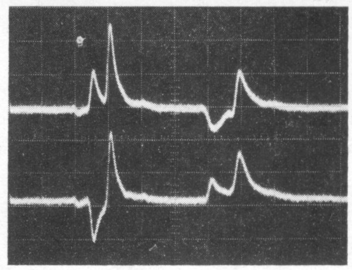

Fig. 41. Same as Fig. 40 but with far end of active and passive lines shorted together.

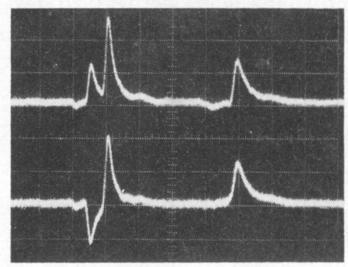

Fig. 42. Same as Fig. 40 but with 120 ohms ($\approx 2Z_{00}$) connected between the far ends of the active and the passive line.

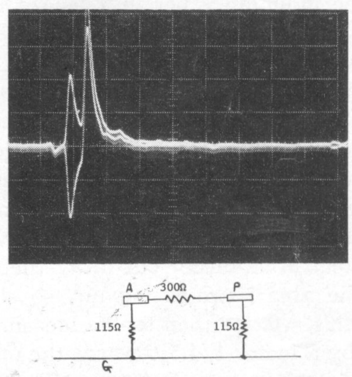

Fig. 43. Same as Fig. 40 but with the two lines terminated in the correct delta of resistors. Vertical scale: Uncalibrated. Horizontal scale: 5 ns/div.

Fig. 44. Same as Fig. 43 but to a different vertical scale.

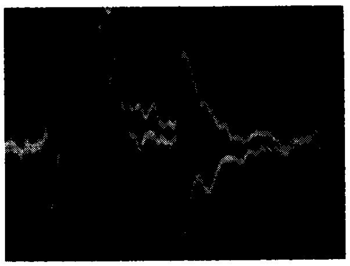

Fig. 45. Same as Fig. 44 but with 300-ohm resistor removed.

IX. Methods of Determining Z_o, Z_{0o}, Z_{0e}, c, c_o, c_e, Fast Crosstalk and Velocity Percent Difference

Resistive Paper

It was found that the easiest way to determine these values was by painting electrodes onto resistive paper to represent a cross section of the two lines and also the voltage plane. (It is possible to avoid the tedium of painting the voltage plane by repeating the image of the conductors below the voltage plane, and leaving the voltage plane out).

The following values can be measured directly: L, the inductance per unit length of a single line above a ground plane, by using a resistance meter and applying the correction factor; μ_0/ρ, where ρ = resistance per square of the paper and μ_0 = the permeability of free space, L_e, the inductance per unit length in the even mode, and L_o, the inductance per unit length in the odd mode, can be measured in a similar way.

It is more difficult to measure capacitance per unit length, because two dielectrics are involved, both air ($\epsilon_r = 1$) and epoxy glass ($\epsilon_r = 4.5$). To get correct measurements, it would be necessary to have resistive paper with $4\frac{1}{2}$ times the resistivity in the region representing air, above the board. This would be very difficult to achieve. Instead, the author cut away the paper completely in the area representing air, so simulating a dielectric with $\epsilon_r = 0$. He then took a measurement, and weighted it by a factor 1/4.5 towards the measurement made before cutting away the paper. The author estimates that in lines of practical dimensions the resulting error for the value of $\mathfrak{C}$, $\mathfrak{C}_e$ and $\mathfrak{C}_o$ is less than 16 percent. Since the important values, Z and c, depend upon the square root of the capacitance, an error of less than 8 percent can be expected in all the values that are of importance.

For parallel lines of the dimensions shown in Fig. 26, resistive paper methods indicated a ratio of $Z_{0e}/Z_{0o} = 1.76$. Fig. 33, indicates a ratio of 1.89.

The greatest inaccuracy will occur in calculation of percent velocity difference between two lines which are closely spaced. The resistive paper results are always on the safe side, indicating a greater velocity difference than actually exists. In the exaggerated case shown in the figures in Section IX, where FX had the unreasonably high value of 31 percent, there was an overestimate of percent velocity difference of some 50 percent. The actual percent velocity difference was 9 percent, but the percent predicted by resistive paper was 15 percent. So the designer who used resistive paper values would be overdesigning. However, in practical cases, where the lines are more widely separated, the discrepancy can be expected to fall off. So in practical cases, the graphs of FX and also DX will have ample accuracy. This is confirmed by the fact that an excellent correlation exists between the graphs of FX and the amplitude of FX that is measured experimentally from fabricated boards when FX is of reasonable (practical) amplitude, say 5 percent or 10 percent.

Calculation

Methods so far devised are not very accurate (reference [16], page 109).

Direct Measurement

Once a board has been fabricated with two long parallel surface lines, it is reasonably easy to send a voltage step down one line and measure the resulting maximum FX on the other line.

So the ratio

$$\frac{\text{max. FX}}{\text{signal}} = \frac{Z_{0e} - Z_{0o}}{Z_{0e} + Z_{0o}}$$

can be determined experimentally. The results agree very well in the 5 percent and 10 percent range with results arrived at by resistive paper.

In this same range, it is not practicable to determine percent velocity difference experimentally, because it is so small. As previously stated in the section on resistive paper, the experimental results for percent velocity difference for closely spaced wires are significantly lower than the values measured with resistive paper. The author recommends that the designer stay on the safe side by using the larger, resistive paper, values for percent velocity difference. These are the ones shown in the graph.

X. Graphic Description of Crosstalk between Surface Lines

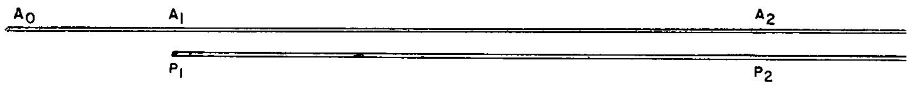

Fig. 46. Plan view of parallel surface conductors.

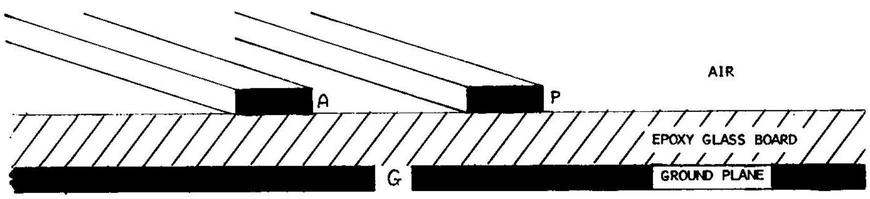

Fig. 47. Cross section of surface active transmission line and passive transmission line.

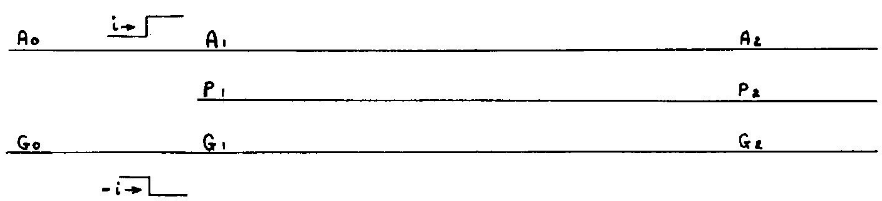

Fig. 48. Diagrammatic representation of active transmission line and passive transmission line.

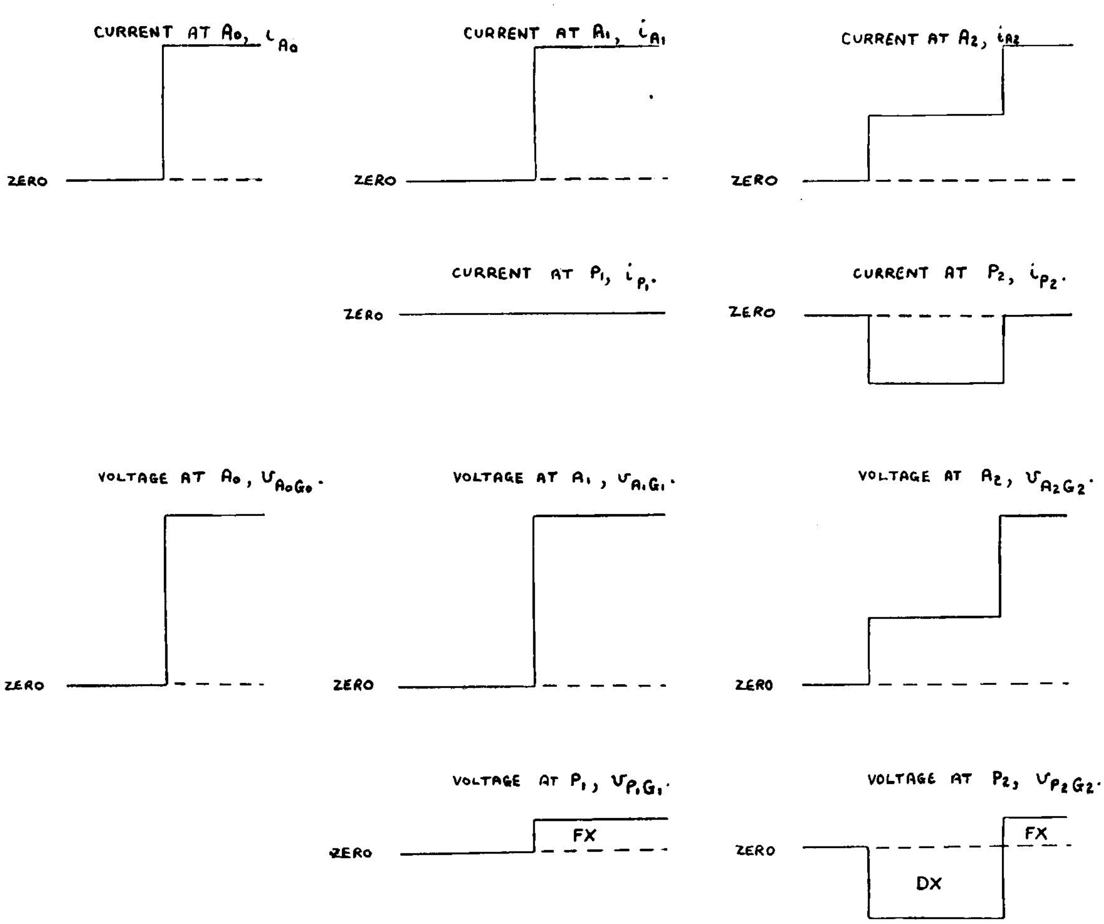

Fig. 49. Signal waveforms at various points down the active and passive lines.

XI. Theory of Crosstalk in Surface Lines

TEM waves are not possible in an inhomogeneous medium (references [7], page 362; [8], page 5.4; [9], page 1651; [10], page 299). However, it is usually assumed that the signal propagation in a surface printed wire above a ground plane is TEM, (reference [11], page 486) and there is some justification for this (reference [8], page 5.6).

If a digital signal is not significantly distorted when it travels down a surface conductor, then the propagation mode must approximate to TEM. A comparison of the steady-state charge density distribution for steady voltage on the line and the current density distribution on the line for minimum magnetic flux per unit current will indicate how much the propagation mode will differ from TEM. With a homogeneous dielectric and conductors of zero resistivity, these two distributions are the same, and propagation is pure TEM. With an inhomogeneous dielectric, these two steady-state distributions will differ. However, during any transient, charge and current distribution must be the same. So after the voltage current transient, there will be redistribution of charge and current about the conductor to meet the necessary steady-state requirements of maximum capacitance and minimum inductance to maximize the energy stored in the line. In the case of a printed wire above a ground, it can be assumed that all three distributions are very similar, so that the redistribution is small, and deviation from TEM propagation is negligible.

Experience that a digital signal travels down a surface conductor with little distortion (rise time degradation) confirms this. Only TEM mode will give propagation without distortion.

The following theory draws on the fine work of M. Cotte of 20 years ago, and is of interest from an historical point of view. However, the new approach in the appendices of this paper is simpler and clearer. The results of the two approaches can be shown to be the same.

The system considered here consists of two parallel conductors on a dielectric board above a ground plane, as shown in Figs. 50 and 25. The partial differential equations describing the system are

$$-\frac{\partial I_1}{\partial x} = C\frac{\partial V_1}{\partial t} - C_m\frac{\partial V_2}{\partial t}$$

$$-\frac{\partial I_2}{\partial x} = -C_m\frac{\partial V_2}{\partial t} + C\frac{\partial V_2}{\partial t}$$

$$-\frac{\partial V_1}{\partial x} = L\frac{\partial I_1}{\partial t} + M\frac{\partial I_2}{\partial t}$$

$$-\frac{\partial V_2}{\partial x} = M\frac{\partial I_1}{\partial t} + L\frac{\partial I_2}{\partial t}$$

(references [17], page 344; [5], page 381; [11], page 486) where C is the capacitance per unit length of each line,

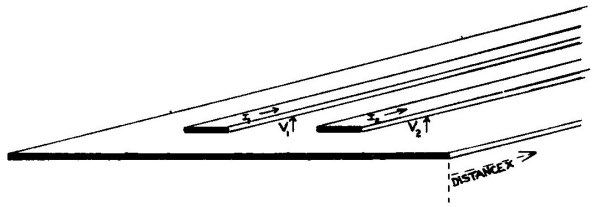

Fig. 50. Diagram of two parallel conductors on a dielectric board above a ground plane.

C_m is the capacitance between the lines, L the inductance per unit length of each line, and M the mutual inductance between the lines. These equations are valid only for a TEM mode of propagation.

To solve these equations, each variable is replaced by its Laplace transform; $L[V_1] = \overline{V}_1$, etc.

$$-\frac{\partial \overline{I}_1}{\partial x} = Cs\overline{V}_1 - C_m s\overline{V}_2 \tag{1}$$

$$-\frac{\partial \overline{I}_2}{\partial x} = -C_m s\overline{V}_1 + Cs\overline{V}_2 \tag{2}$$

$$-\frac{\partial \overline{V}_1}{\partial x} = Ls\overline{I}_1 + Ms\overline{I}_2 \tag{3}$$

$$-\frac{\partial \overline{V}_2}{\partial x} = Ms\overline{I}_1 + Ls\overline{I}_2. \tag{4}$$

Differentiating (3) and (4) and combining them with (1) and (2), results in

$$\frac{\partial^2 \overline{V}_1}{\partial x^2} = (LC - MC_m)s^2\overline{V}_1 + (MC - LC_m)s^2\overline{V}_2 \tag{5}$$

$$\frac{\partial^2 \overline{V}_2}{\partial x^2} = (MC - LC_m)s^2\overline{V}_1 + (LC - MC_m)s^2\overline{V}_2. \tag{6}$$

To simplify the solution, a common mode CM and a differential mode DM of propagation are now defined:

$$\overline{V}_a = \overline{V}_1 + \overline{V}_2 \qquad \overline{I}_a = \overline{I}_1 + \overline{I}_2 \quad \text{CM} \tag{7}$$

$$\overline{V}_b = \overline{V}_1 - \overline{V}_2 \qquad \overline{I}_b = \overline{I}_1 - \overline{I}_2 \quad \text{DM.} \tag{8}$$

Adding and subtracting (5) and (6) results in

$$\frac{\partial^2 \overline{V}_a}{\partial x^2} = (L + M)(C - C_m)s^2\overline{V}_a \tag{9}$$

$$\frac{\partial^2 \overline{V}_b}{\partial x^2} = (L - M)(C + C_m)s^2\overline{V}_b. \tag{10}$$

The solutions of these two differential equations are

$$\overline{V}_a = E_1 e^{s(x/c_e)} + E_2 e^{-s(x/c_e)} \tag{11}$$

$$\overline{V}_b = E_3 e^{s(x/c_o)} + E_4 e^{-s(x/c_o)} \tag{12}$$

where

$$c_e = \frac{1}{\sqrt{(L+M)(C-C_m)}} \quad \text{and} \quad c_o = \frac{1}{\sqrt{(L-M)(C+C_m)}}.$$

It can be shown that when there is a homogeneous medium, $C_m/C = M/L$ and $c_e = c_o$. However, in this case,

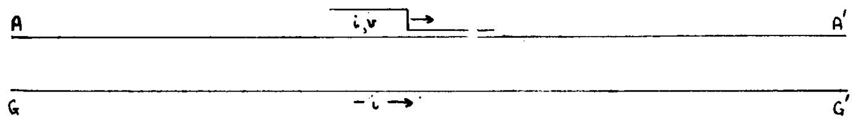

Fig. 51. Diagram of a two wire transmission line.

with both a dielectric board and air the medium is not homogeneous.

To solve for the currents, (11) and (12) are substituted into (3) and (4) to obtain

$$\bar{I}_a = \frac{1}{Z_a}\left[-E_1 e^{s(x/c_e)} + E_2 e^{-s(x/c_e)}\right] \tag{13}$$

$$\bar{I}_b = \frac{1}{Z_b}\left[-E_3 e^{s(x/c_o)} + E_4 e^{-s(x/c_o)}\right] \tag{14}$$

where

$$Z_a = \sqrt{\frac{L+M}{C-C_m}} \quad \text{and} \quad Z_b = \sqrt{\frac{L-M}{C+C_m}}\,.$$

$\bar{V}_1$, $\bar{V}_2$, $\bar{I}_1$ and $\bar{I}_2$ can now be determined at any point on the lines by using the relationships

$$\bar{V}_1 = \tfrac{1}{2}(\bar{V}_a + \bar{V}_b) \qquad \bar{I}_1 = \tfrac{1}{2}(\bar{I}_a + \bar{I}_b) \tag{15}$$

$$\bar{V}_2 = \tfrac{1}{2}(\bar{V}_a - \bar{V}_b) \qquad \bar{I}_2 = \tfrac{1}{2}(\bar{I}_a - \bar{I}_b). \tag{16}$$

Appendix I

Proof that Only One Type of Wave-Front Pattern Can Be Propagated Down a Two-Wire System

In Fig. 51, assume that a current–voltage step i, v, is traveling down the parallel lines AA', GG' from left to right with a velocity c. Assume that no change of current, voltage or electromagnetic fields is taking place except in the plane at right angles to AA' passing through the point where the step is at that moment. At every point to the right of the step, the voltage between the two lines is zero and the current is zero. At every point to the left of the step, the voltage between the two lines is v, the current in AA' is i and the current in GG' is $-i$.

Now use Faraday's law of induction around the loop $AA'G'G$. This later became one of Maxwell's equations (reference [15], page 302). The law states that the total voltage induced around a contour C (in this case $AA'G'G$) is equal to the negative time rate of change of magnetic flux through this contour

$$v_{\text{back EMF}} = -\frac{d\phi}{dt}\,. \tag{17}$$

Now define L as the self-inductance per unit length of the pair of conductors AA' and GG'

$$L = \frac{\phi}{i}\,.$$

Now in time δt, the current step will have traveled a distance δs, where $\delta s/\delta t = c$.

The change of flux in the loop $AA'G'G$ will be

$$\delta\phi = L\delta s \cdot i. \tag{18}$$

Substituting in (17) for $\delta\phi$ brings

$$v_{\text{back EMF}} = -Li\frac{ds}{dt} = -Lic. \tag{19}$$

Now the total voltage around the loop $AA'G'G$ must be zero, by one of Kirchoff's laws.

So there must be an impressed voltage placed across AG where

$$v_{AG} = -v_{\text{back EMF}} = Lic. \tag{20}$$

Equation (20) gives one necessary condition relating voltage, current and velocity for the current step. There is a second condition, which derives from the principle of conservation of electric charge. Current, and therefore charge, is continually entering the conductor AA' at A, and this current charges the line AA' relative to GG' to a voltage v.

Let C be defined as the capacitance per unit length between the conductors AA' and GG':

$$C = \frac{q}{v}\,.$$

Now in a time δt, a quantity of charge $\delta q = i\delta t$ will charge up a length of line δs to a voltage v. The capacitance of this length δs is $C\delta s$. Therefore

$$C\delta s = \frac{i\delta t}{v}\,.$$

Rearranging,

$$v = \frac{i}{Cc}\,. \tag{21}$$

Equations (20) and (21) give the two necessary conditions relating voltage, current and velocity for a current step traveling down two parallel lines.

If (20) is divided by (21),

$$\frac{v}{v} = \frac{LicCc}{i}$$

$$\therefore c = \pm\frac{1}{\sqrt{LC}}\,.$$

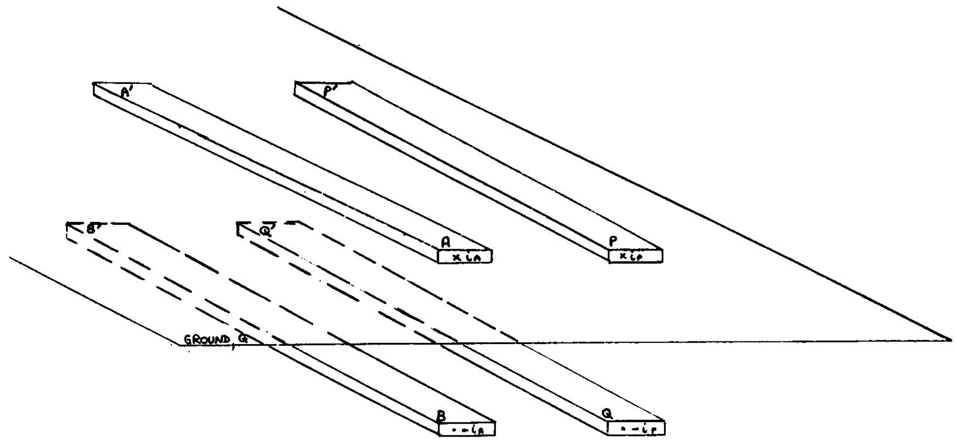

Fig. 52. Diagram of two parallel conductors above a ground plane, and their images.

We neglect the negative solution, because we are interested only in signals traveling from left to right.

$$\therefore C = +\frac{1}{\sqrt{LC}}. \qquad (22)$$

Substituting for c in (20) we get

$$\frac{v}{i} = +\sqrt{\frac{L}{C}} = \text{characteristic impedance } Z. \qquad (23)$$

Conclusion: If a current voltage step v, i, travels down a pair of parallel lines, the following conditions always apply:

$v = iZ$, where Z is a constant for the lines.
$c = 1/\sqrt{LC}$ where L and C are constant for the lines.

Appendix II

Proof that Only Two Types of Wave-Front Patterns Can Be Propagated Down a System of Two Wires and Ground Plane

In Fig. 52, the method of images is used; it is assumed that $i_B = -i_A$, $i_Q = -i_P$. The following terms are defined for steady state conditions:

L = Magnetic flux per unit length between AA' and BB' when unit current flows down AA' and back on BB'.
M = Magnetic flux per unit length between AA' and BB' when unit current flows down PP' and back on QQ'.
C = Charge per unit length on AA' and BB' which produces unit voltage drop between AA' and BB' = 1/coefficient of capacitance.
D = Charge per unit length on AA' and BB' which produces unit voltage drop between PP' and QQ' = 1/coefficient of induction. This could well be called "Mutual Capacitance."

Now assume that a wave front involving current steps i_A and i_P is traveling down the lines with a velocity c.

From $v = d\phi/dt$ between AA' and BB', we get (as in (19)),

$$v_{AB} = Li_A c + Mi_P c. \qquad (24)$$

Similarly $v = d\phi/dt$ between PP' and QQ', so

$$v_{PQ} = Li_P c + Mi_A c. \qquad (25)$$

Also, from $v = q/C$, (as in (21)),

$$v_{AB} = \frac{i_A}{Cc} + \frac{i_P}{Dc} \qquad (26)$$

$$v_{PQ} = \frac{i_P}{Cc} + \frac{i_A}{Dc} \qquad (27)$$

First find c.
Eliminate voltages from (24) through (27).
From (24) and (26),

$$Li_A c + Mi_P c = \frac{i_A}{Cc} + \frac{i_P}{Dc}$$

$$Li_A c^2 + Mi_P c^2 = \frac{i_A}{C} + \frac{i_P}{D}$$

$$\therefore \frac{i_A}{i_P} = -\frac{\left(Mc^2 - \frac{1}{D}\right)}{\left(Lc^2 - \frac{1}{C}\right)}. \qquad (28)$$

Similarly, from (25) and (27),

$$\frac{i_A}{i_P} = -\frac{\left(Lc^2 - \frac{1}{C}\right)}{\left(Mc^2 - \frac{1}{D}\right)}. \qquad (29)$$

Eliminate i_A and i_P from (28) and (29) to get

$$c = \pm \sqrt{\frac{\frac{1}{C} + \frac{1}{D}}{L + M}} \quad \text{or} \quad \pm \sqrt{\frac{\frac{1}{C} - \frac{1}{D}}{L - M}}.$$

So in the forward direction there are two possible velocities of propagation,

$$c_e = + \sqrt{\frac{\frac{1}{C} + \frac{1}{D}}{L + M}}$$

or

$$c_o = + \sqrt{\frac{\frac{1}{C} - \frac{1}{D}}{L - M}}.$$

Returning to (28) and using the results for **c**, we find that the following two wave fronts are possible:

1) EM wave $c_e = \sqrt{\frac{\frac{1}{C} + \frac{1}{D}}{L + M}}$

$$Z_{0e} = \sqrt{(L + M)\left(\frac{1}{C} + \frac{1}{D}\right)}$$

$$i_A = i_P$$
$$v_{AB} = v_{PQ}.$$

2) OM wave $c_o = \sqrt{\frac{\frac{1}{C} - \frac{1}{D}}{L - M}}$

$$Z_{0o} = \sqrt{(L - M)\left(\frac{1}{C} - \frac{1}{D}\right)}$$

$$i_A = -i_P$$
$$v_{AB} = -v_{PQ}.$$

ACKNOWLEDGMENT

The author would like to acknowledge the guidance received from K. Johnson of I.C.T., Manchester, England.

He would like to thank P. Nygaard of Motorola, Phoenix, Ariz., for working out Section XI, and W. Herndon of Fairchild, Palo Alto, Calif., for help with Section I. Dr. J. A. Barkson of A.S.U. also contributed valuable help.

The high-quality printed circuit boards required to give the results shown in this paper were made by H. Hannah, A. Ziolkowski, and R. Gonsalez of Motorola, Phoenix.

REFERENCES

[1] E. C. Garth and I. Catt, "Ultrahigh-speed IC's require shorter, faster interconnections," *Electronics*, vol. 39, pp. 103–110, July 11, 1966.

[2] S. Ramo and J. R. Whinnery, *Fields and Waves in Modern Radio*, 2nd ed. New York: Wiley 1953.

[3] S. B. Cohn, "Shielded coupled-strip transmission line," *IRE Trans. Microwave Theory and Techniques*, vol. MTT-3, pp. 29–38, October 1955.

[4] B. M. Oliver, "Directional electromagnetic couplers," *Proc. IRE*, vol. 42, pp. 1686–1692, November 1954.

[5] M. Cotte, "Ondes de courant sans tension et de tension sans courant sur deux lignes parallelles," *L'Onde Electrique*, vol. 34, pp. 381–383, 1954.

[6] W. J. Getsinger, "Coupled rectangular bars between parallel plates," *IRE Trans. Microwave Theory and Techniques*, vol. MTT-10, pp. 65–72, January 1962.

[7] W. L. Weeks, *Electromagnetic Theory for Engineering Applications*. New York: Wiley, 1964.

[8] A. M. Shah, "Propagation characteristics of inhomogeneous multiconductor transmission lines," 6th International Electronic Circuit Packaging Symposium, August 1965, pp. 5.1–5.19, published by *Electronic Design News*.

[9] F. Assadourian and E. Rimai, "Simplified theory of microstrip transmission systems," *Proc IRE*, vol. 40, pp. 1651–1657, December 1952.

[10] T. T. Wu, "Theory of microstrip," *J. Appl. Phys.*, vol. 28, p. 299, March 1957.

[11] D. B. Jarvis, "The effects of interconnections on high-speed logic circuits," *IEEE Trans. Electronic Computers*, vol. EC-12, pp. 476–487, October 1963.

[12] S. A. Schelkunoff, *Electromagnetic Waves*. New York: D. Van Nostrand, 1943.

[13] S. B. Cohn, "Problems in strip transmission lines," *IRE Trans. Microwave Theory and Technique*, vol. MTT-3, pp. 119–126, March 1955.

[14] G. L. Matthaei, L. Young, and E. M. T. Jones, *Microwave Filters, Impedance-Matching Networks, and Coupling Structures*. New York: McGraw-Hill, 1964.

[15] R. Plonsey and R. E. Collin, *Principles and Applications of Electromagnetic Fields*. New York: McGraw-Hill, 1961.

[16] A. Schwarzmann, "Microstrip plus equations adds up to fast designs," *Electronics*, vol. 40, pp. 109–112, October 2, 1967.

[17] M. Cotte, "Théorie de la propagation d'ondes de choc sur deux lignes parallèles," *Rev. Gen. Elec.*, vol. 56, pp. 343–350, 1947.